A Low-loss Wideband Filtering Coupler with Patterned Substrate Integrated Suspended Line (SISL) Technology

Li Ma [1], Yongle Wu[*1], Mingxing Li [2], Weimin Wang [2], and Yuanan Liu [2]

[1] State Key Laboratory of Information Photonics and Optical Communications, School of Electronic Engineering
Beijing University of Posts and Telecommunications, Beijing, 100876, China
mali2013@bupt.edu.cn, wuyongle138@gmail.com

[2] Department of Electronic Engineering, Beijing Key Laboratory of Work Safety Intelligent Monitoring
Beijing University of Posts and Telecommunications, Beijing, 100876, China
lmxdx1990@163.com, wangwm@bupt.edu.cn, yuliu@bupt.edu.cn

Abstract ─ A wideband filter-integrated coupler has been presented using the substrate integrated suspended line structure with patterned substrate. This coupler is composed of a two-line coupled line, two variant coupled lines, and four three-line coupled lines at each port. The SISL structure is composed of five print circuit boards, connected together by metal via holes. There is a hollowed substrate between two air cavities to reduce the loss. For further explanation, two wideband filtering SISL couplers operating at different operating frequencies with equal/unequal power divisions are designed and simulated, of which a specific coupler working at 1.66 GHz with a relative bandwidth of about 52.56% is fabricated and measured. The experimental results agree well with the theoretical and simulation ones. This proposed coupler has many advantages such as self-packaged, low loss, filter integration, arbitrary power division ratio, and inherent DC-block function.

Index Terms ─ Filtering coupler, microwave components, patterned substrate, substrate integrated suspended line (SISL), wide band.

I. INTRODUCTION

Branch-line coupler (BLC) has become an essential part in the RF/microwave circuits and systems, which has found a wide utilization in balanced power amplifier [1], balanced mixer [2], and frequency discriminator [3]. Nowadays, with the rapid development of 5G and satellite communication, multiple-antenna systems, such as isophoric sparse arrays [4] and massive MIMO arrays [5], have brought forward higher requirements on the feed network of antenna and antenna array. As a critical part of the feed network, BLC has been used for Butler matrix for beam forming network [6], exciting multiple modes of the multimode multi-element antenna [7], and so on. Thus, multi-function integration, such as filtering, power splitting/combining, unequal power-division ratio, flatness of amplitude and phase differences, has been more and more important for application, among which the filtering-integrated coupler has attracted more and more interests of researchers. The conventional method to realize filtering function is cascading filtering units with the coupler, for example, reference [8] uses net-type resonator to construct a rat-race coupler with bandpass response, and reference [9] utilized coupled resonator to design the filtering 180º hybrid. Recently, other technologies like substrate integrated waveguide (SIW) [10] and low temperature co-fired ceramic (LTCC) [11] are also introduced into the design of filtering coupler. But the aforementioned design methods cannot realize broad bandwidth, filtering function and low loss property at the same time.

The substrate integrated suspended line (SISL) structures [12-13] are composed of multi-layer print circuit boards. There are two air cavities on both sides of the core circuit, so the field of the circuit is mainly distributed in the air. Besides, the substrate of the core circuit is hollowed with specific shape. Thus, both the dielectric loss and the radiation loss of the suspended line are relatively smaller than the ones of microstrip line (ML) and strip line. In [12], a novel compact branch-line coupler has been designed using the SISL technology, and in [13], SISL and double-sided SISL (DSISL) inductors with patterned substrate are proposed. Compared with conventional metal-cavity structure, SISL technology has solved many problems, showing an excellent performance on cost, weight, support of the substrate, and so on.

In this paper, a wideband filter-integrated coupler using substrate integrated suspended line (SISL) technology has been designed, simulated, and fabricated. As an expansion of the authors' previous work in [14], we chose two specific couplers as examples to further explain the design and advantages of the SISL coupler. This coupler improved the origin transmission-line

Submitted On: September 25, 2018
Accepted On: December 27, 2018

structure in [15] for size reducing. Besides, with the help of the patterned SISL technology, loss can be narrowed. And the comparison of the losses between the proposed one and conventional one is also given. This low-loss SISL coupler can also realize filter integration, flexible power division ratio, and inherent DC-block function at the same time. Compared with the former work of the authors in [14], this work explains the design procedures in detail and provides two design examples with experimental result, in which the properties of this coupler such as low loss, flexible power division ratio, etc. have been verified. Besides, we discuss the influence of physical circuit parameters on the properties of the coupler and give the design procedures. The first SISL coupler named *Example A* works at 1.66 GHz with 7 dB power division, and the other named *Example B* is designed with 3.50 GHz operating frequency and equal power division. Both simulation and measured results coincide well with each other. Moreover, this low-loss wideband filtering BLC can be applied to many situations of wireless communication systems.

II. WIDEBAND FILTERING SISL COUPLER

The design method of the proposed wideband filter-integrated coupler can be divided into two parts. Firstly, we design and optimize the SISL structure according to the technology in [12]. Secondly, the basic circuit of the wideband filtering coupler is designed and discussed. Finally, we combine these two procedures together and take the overall simulation and optimization of the SISL coupler.

A. SISL structure

The SISL structure contains five double-side print circuit boards, which are fixed together by several screws as shown in Fig. 1. The five substrate layers, named as *Substrate* 1, 2, 3, 4, and 5, have created totally ten metal planes named as *G*1, *G*2, …, *G*10 from top to bottom. *Substrate* 1 and 5 act as electromagnetism shields for the SISL structure, with *G*1, 2, 9, and 10 being ground planes. *Substrate* 2 and 4 provide two air cavities on the upper and lower of the suspended circuit. The air cavities are actually a kind of open slot of the substrate, which are surrounded by via holes. *Substrate* 3 acts as the suspended substrate. The basic circuit of the wideband filtering coupler, which would be discussed in the next part, is etched on *G*5. The field of the circuit on *G*5 is mainly distributed on the two air cavities on *Substrate* 2 and 4, with a boundary brought by the metal holes surrounding the air cavities. The dielectric of *Substrate* 3 possesses low loss tangent and is hollowed according to the shape of the coupler, thus both radiation loss and substrate loss can be greatly reduced [13].

B. Core circuit of the wideband filtering coupler

The primary circuit of the broadband filter-integrated coupler on *G*3 is shown in Fig. 2. The coupler has both horizontally and vertically symmetric layout, composed of one two-line coupled line in the center, two deformed coupled lines at the top and bottom sides, and four three-line coupled lines connected to the ports. The coupler can also achieve wideband filtering function, inherent DC-block between the ports, and unequal power division. The power division ratio can be altered by tuning w_1 and w_2. For further explanation, two design examples with different design requirements have been designed and simulated.

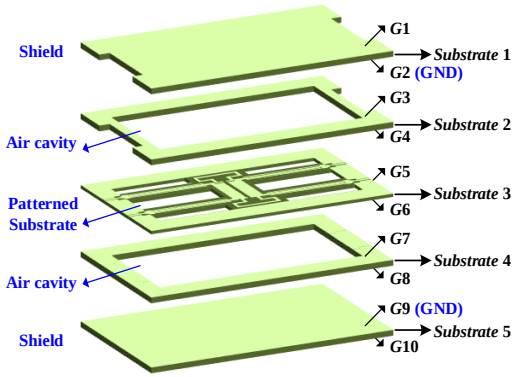

(a)

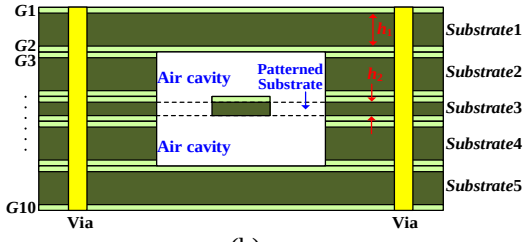

(b)

Fig. 1. The SISL construction of the proposed coupler: (a) 3D layout and (b) cross section.

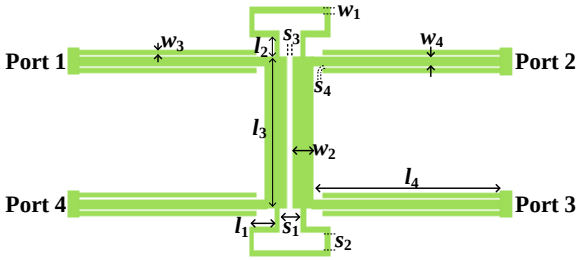

Fig. 2. The circuit configuration of the wideband filtering coupler.

III. DESIGN EXAMPLES

A. Example A

The first case of the SISL coupler named *Example A* works at 1.66 GHz with 7 dB power division, which

has been discussed in [14]. The material of *Substrate* 1, 2, 4, and 5 is chosen as FR-4, with the dielectric constant ε_r being 4.4, the thickness h_1 being 1.5 mm, and loss tangent being 0.02. *Substrate* 3 is designed to be F4B, whose dielectric constant ε_r being 2.65, the thickness h_2 being 0.254 mm, and loss tangent being 0.001.

When designing the specific structure of the SISL coupler, we define the demands of the coupler first, namely operating frequency and power division ratio. The operating frequency of the coupler is related to the lengths of the coupled lines. When the working frequency of a specific coupler is determined, the lengths of l_1, l_2, l_3, and l_4 can be defined. Considering that the power division ratio is affected mainly by the width of w_1 and w_2, they can be determined by repeated simulations using ADS Momentum. Then other parameters will be chosen by the optimization of HFSS Optimetrics Analysis.

Then the physical parameters of the *Example A* can be defined as follows (with units of mm): w_1=1, l_1=3.5, l_2=3, s_1=2, s_2=2, w_2=5, l_3=30, s_3=0.2, w_3=0.8, w_4=1.4, l_4=33, s_4=0.2, w_a=33, l_a=8, w_b=35, l_b=19, w_c=85.8, l_c=52. The structure of *Example A* is illustrated in Fig. 3, in which the total configuration of the SISL structure is shown in Fig. 3 (a), while the circuit of the coupler is shown in Fig. 3 (b). The simulated results are given in Fig. 4 [14]. From these curves, we can see that this coupler can realize wideband filtering function and possesses flat phase difference. The relative bandwidth is about 52.56% with S_{11} lower than -15 dB.

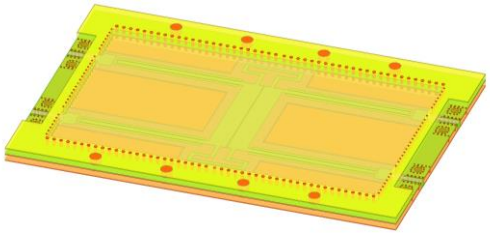

(a)

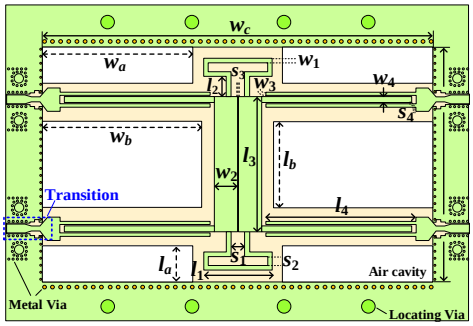

(b)

Fig. 3. The constructions of *Example A*. (a) The overall structure, and (b) the main circuit of the coupler on *G*3.

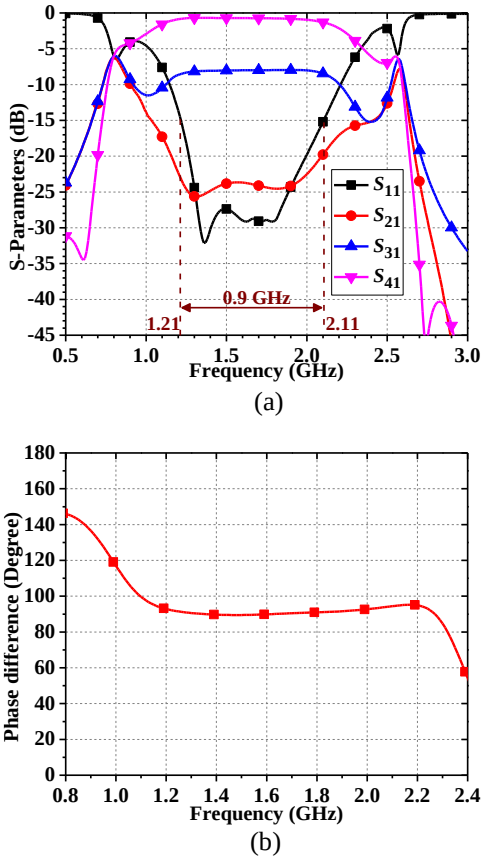

(a)

(b)

Fig. 4. The calculated results of *Example A* [14]. (a) The S-parameters, and (b) phase difference.

The loss of the coupler can be defined as [12],

$$Loss = 1 - |S_{11}|^2 - |S_{21}|^2 - |S_{31}|^2 - |S_{41}|^2. \quad (1)$$

Then we calculate the losses of the designed SISL coupler and conventional microstrip line coupler, which are shown in Fig. 5 [14] for comparison. As we can see, the SISL coupler has a lower loss than the microstrip line one.

The relationship between the power division ratio and the line width of w_1 and w_2 would be further discussed. As shown in Fig. 6, as the increasing of w_1, the power division ratio will decrease. While in Fig. 7, the variation trend of the power division ratio along with the line width w_2 is contrary to the one in Fig. 6. That is, the power division ratio increases with the increasing of the line width w_2.

B. Example B

When designing *Example B*, equal power division and higher operating frequencies are considered. The substrate and configuration of the multi-layer structure are chosen to be the same as those in *Example A*. The physical parameters of the *Example B* can be simulated and optimized by ADS Momentum and HFSS as follows

(with units of mm): w_1=2.5, l_1=3, l_2=2, s_1=2, s_2=1.7, w_2=3.5, l_3=17, s_3=0.2, w_3=0.8, w_4=1.3, l_4=20, s_4=0.2, w_a=20, l_a=8, w_b=22, l_b=12.5, w_c=57.8, l_c=37.4. The SISL structure of the *Example B* is shown in Fig. 8 (a), while the circuit of the coupler is shown in Fig. 8 (b).

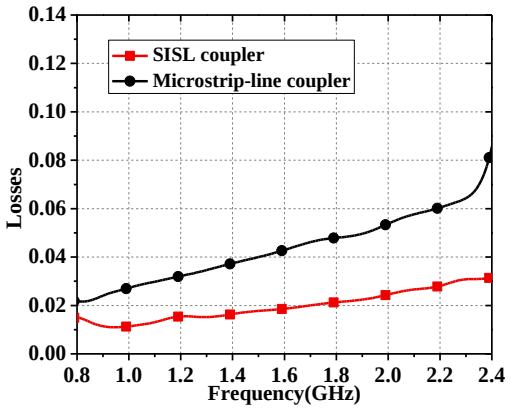

Fig. 5. The losses of SISL coupler and ML coupler [14].

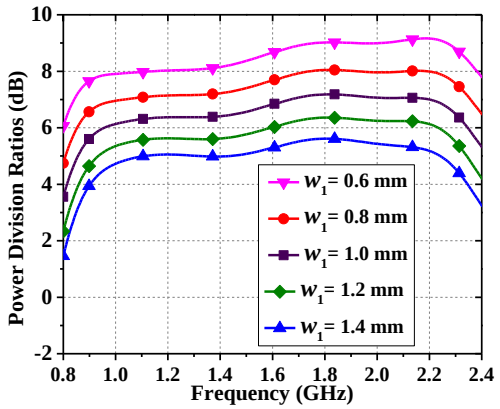

Fig. 6. The power division ratios of the SISL coupler width varies w_1 when w_2 = 5 mm.

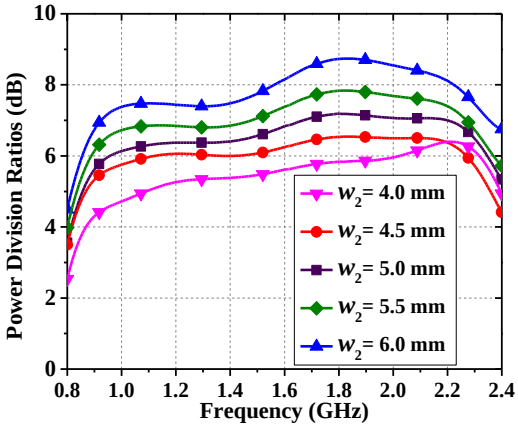

Fig. 7. The power division ratios of the SISL coupler width varies w_2 when w_1 = 1 mm.

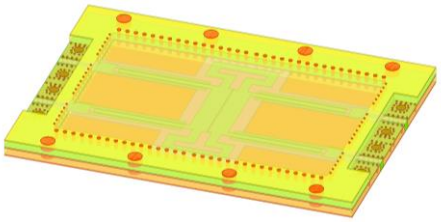

(a)

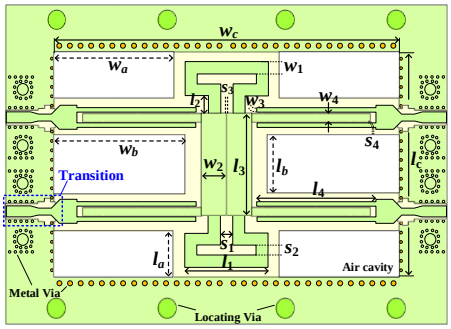

(b)

Fig. 8. The constructions of *Example B*. (a) The overall structure, and (b) the main circuit of the coupler on *G*3.

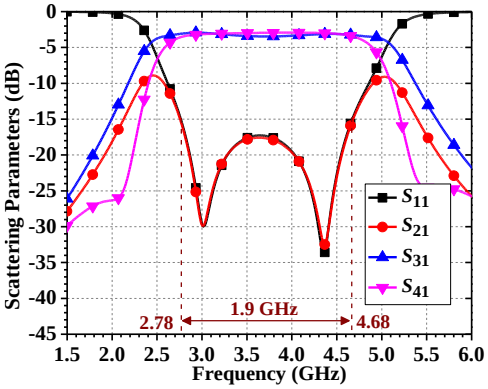

(a)

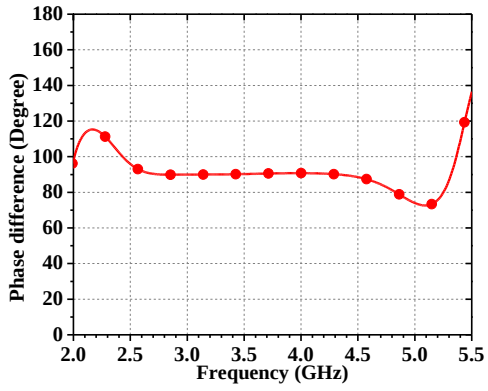

(b)

Fig. 9. The calculated results of *Example B*. (a) The S-parameters, and (b) phase difference.

The simulated scattering parameters and phase difference are shown in Figs. 9 (a) and (b), respectively. It can be observed that this coupler possesses a relative bandwidth of 54.28% with S_{11} lower than -15 dB and a flat phase difference. So, the wideband filtering coupler has been realized.

IV. MEASURED RESULTS

In order to verify the performance of the SISL wideband filer-integrated coupler, we take *Example A* as an experimental case. The design parameters of the coupler are all the same as those explained in Section III.A. The photograph of the fabricated SISL coupler is illustrated in Fig. 10. The size of the coupler is about 110.2×70×6.254 mm^3. Figures 11 (a) and (b) are the simulated and measured S-parameters and phase differences of the coupler in *Example A*, separately. As we can see from the figures, the coupler works at 1.66 GHz, with a power division of about 7 dB. The coupler has good matching and isolation and possesses a relative bandwidth of about 49.398% with S_{11} lower than -15 dB. In addition, the major features and advantages of this SISL wideband filtering BLC compared with other reported ones are listed in Table 1.

V. CONCLUSION

In this paper, a compact wideband filter-integrated coupler is designed, simulated and fabricated using the patterned substrate integrated suspended line technology. The design and optimization procedures of the coupler have been explained in detail, and two cases with different operating frequencies of 1.66/3.5 GHz and unequal/equal power division ratios were designed as examples. The loss of the designed couplers was greatly reduced compared with that of traditional ones. Then for further verification, a specific SISL coupler working at 1.66 GHz with 7 dB power division and 52.56% relative bandwidth was designed and fabricated. The measured scattering parameters and phase difference coincided well with the theory and the simulated results. This coupler has the advantages such as self-package, low loss, filter integration, and flexible power division ratio, which is propitious to the applications in the microwave circuits and wireless communication systems.

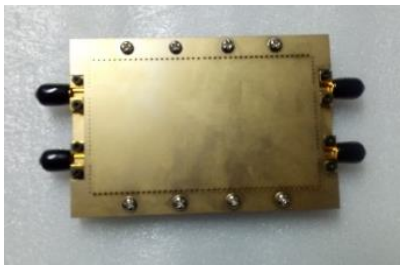

Fig. 10. The photograph of the SISL coupler.

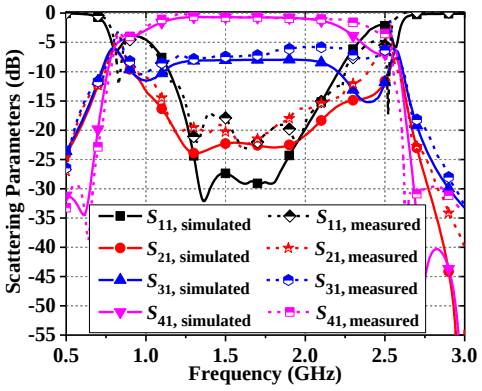

(a)

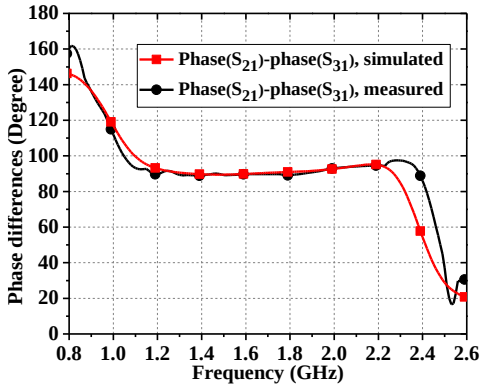

(b)

Fig. 11. The simulated and measured results of the wideband filtering SISL coupler. (a) The S-parameters, and (b) phase difference.

Table 1: Performance comparison of the proposed SISL wideband filtering BLC with other reported ones

Refs.	BW*	IL (dB)	Technology	Self-Packaged
[8]	19%	1.38	PCB	No
[9]	10%	0.7	PCB	No
[10]	2.5%	1.9	SIW	No
[11]	8.6%	1.8	LTCC	Yes
This work	49.398%	0.655	SISL	Yes

*: with return loss < -15 dB.

ACKNOWLEDGMENT

This work was supported in part by National Natural Science Foundations of China (No. 61671084, and No. 61821001), Guangzhou Major Projects of Industrial Technology of China (Research and Development of Large-scale Multi-beam Antenna Array for 5G Massive MIMO Communication). This paper is an expanded version from the International Applied Computational Electromagnetics Society (ACES) Symposium, Beijing, China, July 2018 [14].

REFERENCES

[1] A. Grebennikov, *RF and Microwave Power Amplifier Design*. New-York: McGraw-Hill, 2015.

[2] H. Ebrahimian, M. Ojaroudi, N. Ojaroudi, and N. Ghadimi, "Distributed diode single-balanced mixer using defected and protruded structures for doppler radar applications," *Applied Computational Electromagnetics Society (ACES) Journal*, vol. 30, no. 3, pp. 313-318, Mar. 2015.

[3] S. Moon, I. Yom, and H. Lee, "K-band phase discriminator using multiport downconversion for monopulse tracker," *IEEE Microw. Wireless Compon. Lett.*, vol. 27, no. 6, pp. 599-601, June 2017.

[4] A. F. Morabito and P. G. Nicolaci, "Optimal synthesis of shaped beams through concentric ring isophoric sparse arrays," *IEEE Antennas Wireless Propag. Lett*., vol. 16, pp. 979-982, Oct. 2017.

[5] B. Yang, Z. Yu, Y. Dong, J. Zhou, and W. Hong, "Compact tapered slot antenna array for 5G millimeter-wave massive MIMO systems," *IEEE Trans. Antennas Propag*., vol. 65, no. 12, pp. 6721-6727, Dec. 2017.

[6] S. Karamzadeh, V. Rafii, M. Kartal, and B. Virdee, "Modified circularly polarised beam steering array antenna by utilised broadband coupler and 4×4 butler matrix," *IET Microw., Antennas Propag.*, vol. 9, no. 9, pp. 975-981, June 2015.

[7] D. Manteuffel and R. Martens, "Compact multimode multielement antenna for indoor UWB massive MIMO," *IEEE Trans. Antennas Propag*., vol. 64, no. 7, pp. 2689-2697, July 2016.

[8] W.-H. Wang, T.-M. Shen, T.-Y. Huang, and R.-B. Wu, "Miniaturized rat-race coupler with bandpass response and good stopband rejection," in *IEEE MTT-S Int. Microw. Symp. Dig.*, Boston, MA, USA, pp. 709-712, June 2009.

[9] C. Lin and S. Chung, "A compact filtering 180˚ hybrid," *IEEE Trans. Microw. Theory Tech*., vol. 59, no. 12, pp. 3030-3036, Dec. 2018.

[10] Y. Cheng and Y. Fan, "Compact substrate-integrated waveguide bandpass rat-race coupler and its microwave applications," *IET Microw. Antennas Propag.*, vol. 6, no. 9, pp. 1000-1006, June 2012.

[11] K. Wang, X. Liu, Y. Li, L. Lin, and X. Zhao, "LTCC filtering rat-race coupler based on eight-line spatially-symmetrical coupled structure," *IEEE Access*, vol. 6, pp. 262-269, 2018.

[12] Y. Wang, K. Ma, and S. Mou, "A compact branch-line coupler using substrate integrated suspended line technology," *IEEE Microw. Wireless Compon. Lett.*, vol. 26, no. 2, pp. 95-97, Feb. 2016.

[13] L. Li, K. Ma, and S. Mou, "Modeling of new spiral inductor based on substrate integrated suspended line technology," *IEEE Trans. Microw. Theory Tech.*, vol. 65, no. 8, pp. 2672-2680, Aug. 2017.

[14] L. Ma, Y. Wu, C. He, W. Wang, and Y. Liu, "A wideband filter-integrated coupler using substrate integrated suspended line (SISL) technology with patterned substrate," in *International Applied Computational Electromagnetics Society (ACES) Symposium*, July 2018.

[15] Y. Wu, L. Jiao, Y. Du, and Y. Liu, "Wideband filter-integrated coupled-line coupler with unequal power division and inherent DC-block function," *Microw. Opt. Technol. Lett.*, vol. 58, no. 1, pp. 121-123, Jan. 2016.

Li Ma received the B.S. degree in Electronic Science and Technology from Beijing University of Posts and Telecommunications (BUPT), Beijing, China, in 2017, where she is currently pursuing the Ph.D. degree. In September 2017, she started her research as a graduate at BUPT. Her research interests include microwave passive components and multi-layer technology.

Yongle Wu received the B.Eng. degree in Communication Engineering and the Ph.D degree in Electronic Engineering from Beijing University of Posts and Telecommunications (BUPT), Beijing, China, in 2006 and 2011, respectively. From April to October in 2010, he was a Research Assistant at the City University of Hong Kong, Kowloon, Hong Kong. In 2011, he joined the BUPT and becomes currently a Full Professor in the School of Electronic Engineering. His research interests include microwave components and wireless systems design.

Mingxing Li received his B.S. degree in College of Information Science and Technology from Henan University of Technology (HAUT), Zhengzhou, China, in 2015. In September 2015, he started his research as a graduate at BUPT and is currently working toward the Ph.D. degree at the same university. His research interests include microwave passive components, RF and radar systems.

Weimin Wang received the B.S. degree in Communication Engineering, the M.S. degree in Electromagnetic Field and Microwave Technology and the Ph.D degree in Electronic Science and Technology from Beijing University of Posts and Telecommunications (BUPT), Beijing, China, in 1999, 2004 and 2014, respectively. In 2014, she joined BUPT. She is currently a Lecturer in the School of Electronic Engineering, BUPT. Her research interests include electromagnetic field and MIMO OTA measurement.

Yuanan Liu received the B.E., M.Eng., and Ph.D. degrees in Electrical Engineering from University of Electronic Science and Technology of China, Chengdu, China, in 1984, 1989 and 1992, respectively. In 1984, he joined the 26th Institute of Electronic Ministry of China to develop the inertia navigating system. In 1992, he began his first Post-doctor position in EMC lab of Beijing University of Posts and Telecommunications (BUPT), Beijing, China. In 1995, he started his second Post-doctor in Broadband Mobile Lab of Department of System and Computer Engineering, Carleton University, Ottawa, Canada. From July, 1997, as Professor, he is with Wireless Communication Center of College of Telecommunication Engineering, BUPT, Beijing, China, where he is involved in the development of next-generation cellular system, wireless LAN, Bluetooth application for data transmission, EMC design strategies for high speed digital system, and Electromagnetic interference (EMI) and Electromagnetic Susceptibility (EMS) measuring sites with low cost and high performance.